Int. J. Electrochem. Sci., 15 **(2020)** 9282 – 9293, doi: 10.20964/2020.09.07

International Journal of
ELECTROCHEMICAL
SCIENCE
www.electrochemsci.org

Enhancement of electrochemical performance of $LiCoO_2$ cathode material at high cut-off voltage (4.5 V) by partial surface coating with graphene nanosheets

Jixian Wang, Nan Wang, Wenzheng Nan, Chen Wang, Xiang Chen, Xin Qi, Shaojiu Yan[*], *Shenglong Dai*

Beijing Institute of Graphene Technology Co. Ltd., AECC Beijing Institute of Aeronautical Materials, Beijing 100095, PR China
[*]E-mail: shaojiuyan@126.com

Received: 25 April 2020 / *Accepted:* 17 June 2020 / *Published:* 10 August 2020

$LiCoO_2$ cathodes suffer from severe side reactions and rapid capacity fading under high-voltage operation. In this study, partial coating of $LiCoO_2$ by small size graphene nanosheets was achieved to experimentally investigate the graphene modification mechanism in improving the electrochemical performances of $LiCoO_2$ cathode under 4.5V cut-off voltage. Compared with pristine $LiCoO_2$, G-LCO exhibited better cycling stability and rate capability between 2.5 and 4.5 V vs. Li^+/Li. Further investigation demonstrated that partial coating with graphene nanosheets could effectively suppress the increase of cell impedance and alleviate the growth of cathode electrolyte interphase(CEI), leading to an outstanding electrochemical performance. This study gives new insights on enhancing cycling stability and rate capability of $LiCoO_2$ under high cut-off voltage.

Keywords: $LiCoO_2$, partial coating, graphene nanosheets, CEI layer, high voltage

1. INTRODUCTION

Among various cathode materials, $LiCoO_2$-based cathode materials have been the most popular in portable electronic devices, due to their good rate capability, ease of production and long cycle life[1-7]. Although $LiCoO_2$ possesses a theoretical specific capacity as high as 274 $mAh \cdot g^{-1}$, commercial $LiCoO_2$ materials only achieve half or little more than half of their theoretical capacity, with a cut-off voltage of 4.2V[8-10]. When charging above 4.2 V vs. Li^+/Li, $LiCoO_2$ materials usually encounter dramatic performance degradation [11-14].

A series of side reactions in bulk and on the surface of $LiCoO_2$ were suggested to be one key factor for rapid capacity fading under high cut-off voltage above 4.2V[15-18]. The sustained growth of cathode electrolyte interface (CEI) resulting from irreversible interfacial reaction and degradation of the

electrolyte has been detected by many groups, which is considered as a significant inducement for performance decay of cathode materials[19-23]. For $LiCoO_2$ at high cut-off voltage above 4.3 V[22-26], the high valence cobalt ions exposed on edge planes and released O_2 at high voltage are attributed for catalyzing the oxidative decomposition of electrolyte[27-29], and thereby intensifying the growth of CEI and fast performance degradation. Improved electrochemical performance has been achieved by coating $LiCoO_2$ with inorganics such as Al_2O_3[30,31], $AlPO_4$[32]and TiO_2[33], which acts as an inert layer between the active sites and electrolytes to suppress the decomposition of electrolytes and dynamic evolution of the CEI layer[27,34]. Unfortunately, the electrical conductivity of the as-mentioned metal oxides and inorganics is usually very low and the amount of coating inorganics must be carefully controlled to ensure a better performance.

Surface coating with conductive carbon has been proven to be highly effective in improving the electrochemical performance of $LiFePO_4$ materials [35,36]. However, since $LiCoO_2$ is prone to be reduced to CoO or Co_3O_4 during typical pyrolytic decomposition of carbon sources[37], there are insufficient reports on carbon coating of $LiCoO_2$[38-40].

Graphene is one kind of two-dimensional carbon materials, which has attracted considerable attention in constructing hybrid cathode materials for lithium-ion batteries due to its high electrical conductivity, good flexibility and stable chemical stability[41-44]. However, in graphene-based electrode, lithium ion transport path tends to be prolonged[43,45], and the "barrier effect" is found to be more severe with an increase in the size of graphene[46]. Therefore, an ideal graphene coating structure for high performance cathode materials should provide a balance between increased electron transport and fast ion diffusion[45-49]. In this study, we designed and realized the G-LCO composite by partially coating $LiCoO_2$ with small size graphene nanosheets. The structure, morphology and electrochemical properties of the G-LCO composite were investigated. Primary electrochemical results showed that the partial coating described in the present work effectively improves the cycling stability and rate capability of $LiCoO_2$ under 4.5 V cut-off voltage.

2. EXPERIMENTAL

2.1 Preparation of $LiCoO_2$-graphene composite

Graphene nanosheets used in this study were prepared using a large scale mechanical exfoliation method from graphite powder in N-methyl-2-pyrrolidone (NMP) as solvent as reported elsewhere[50]. For the preparation of G-LCO composite, 0.02g of as-prepared graphene and 0.98 g of commercial $LiCoO_2$ were ground in a mortar for 20 min. Subsequently, the mixture was dispersed in 50 mL ethanol with ultrasonication for 1h. After careful control of stirring speed for 5h, the mixed solution was slowly evaporated at 90 ℃ under an N_2 atmosphere. Finally, the obtained G-LCO composite was dried in vacuum at 80 ℃ for 10 h to remove moisture.

2.2 Structure and morphology characterizations

Crystal structures of all materials were characterized using a powder X-ray diffraction machine (XRD, Bruker D8 Advance with Cu-Kα radiation). Diffraction data was collected at a scan rate of 2°/min in the 2θ range of 10°-80°. Morphologies of $LiCoO_2$ and G-LCO were investigated using a scanning electron microscope (FE-SEM, FEI Nova NanoSEM 450). Surface properties of $LiCoO_2$ and G-LCO cathodes after cycling at 0.1C for 100 cycles were revealed by X-ray photoelectron spectroscopy(XPS, Thermo ESCALAB 250Xi) with a monochromatized Al Kα X-ray source at etching depth of 0, 10nm, 20nm and 30nm. For all XPS characterizations, the batteries were disassembled and washed in DMC in an argon-filled glove box. Thermogravimetric analysis (TGA) was applied to determine the graphene content on a STA499-F3 NETZSCH thermal analyzer in an air atmosphere from room temperature to 800°C at 5℃/min.

2.3 Electrochemical characterizations

To investigate the electrochemical properties, all the samples were examined using 2032 type coin cells, which were composed of a cathode and a lithium foil anode separated by porous polypropylene film(Celgard 2400). The G-LCO cathode was prepared by mixing G-LCO materials, Super P (SP) and polyvinylidene fluoride (PVDF) at a weight ratio of 81.6: 8.4: 10 in a n-methyl-2-pyrrolidone (NMP) solution to form a homogeneous slurry. The obtained slurry was coated on an aluminum foil followed by drying over night at 120 °C. For comparison, the $LiCoO_2$ cathode was also prepared by mixing $LiCoO_2$ materials, SP and PVDF at a weight ratio of 80: 10: 10 using the same procedures. Then the as-prepared electrodes were pressed and punched into round pieces with 12 mm diameter, with a typical active material loading of 11mg cm^{-2}. The electrolyte was 1.0 mol L^{-1} $LiPF_6$ in a mixed solution of ethylene carbonate (EC) and dimethyl carbonate (DMC) (1:1,by volume) and all the half cells were assembled in an argon-filled glove box. Galvanostatic charge/discharge test was performed by the LAND battery program-control test system (CT2001 A, Wuhan LAND Electronic Co., Ltd., China) between 2.5 and 4.5 V vs. Li+/Li at a current density of 18 mA g^{-1} (0.1C). Cyclic voltammogram (CV) and electrochemical impedance spectroscopy (EIS) measurements were carried out on a electrochemical workstation (Zahner-Zennium, Germany). CVs were measured between 2.5 and 4.5 V (vs. Li^+/Li) with a scanning rate of 0.5 mV s^{-1}. EIS measurements were carried out for cells fresh assembled and after 100 cycles at 0.1C with an amplitude of 5 mV in frequency range from 10 mHz to 100 kHz. All the measurements were performed at ambient temperature (25 ± 3 ℃).

3. RESULTS AND DISCUSSION

Fig. 1 shows the XRD patterns of pristine $LiCoO_2$ and the as-obtained G-LCO. All the reflections of $LiCoO_2$ and G-LCO can be easily assigned to well-ordered hexagonal α-$NaFeO_2$ layered structure with *R-3m* space group. The splitting peaks of (006)/(102) and (018)/(110) are clearly identified, suggesting high purity and a well-ordered layered-structure. The intensity ratios of I(003)/I(104) and

(I(006) + I(102))/I(101) remained approximately the same, indicating that the employed graphene coating process does not change the crystal structure of pristine $LiCoO_2$. Notably, the small hump at approximately 26° in the XRD patterns of G-LCO can be attributed to the (002) reflection of graphite, which indicates the existence of graphene. In addition, no impurity phases were detected in the XRD patterns of both samples.

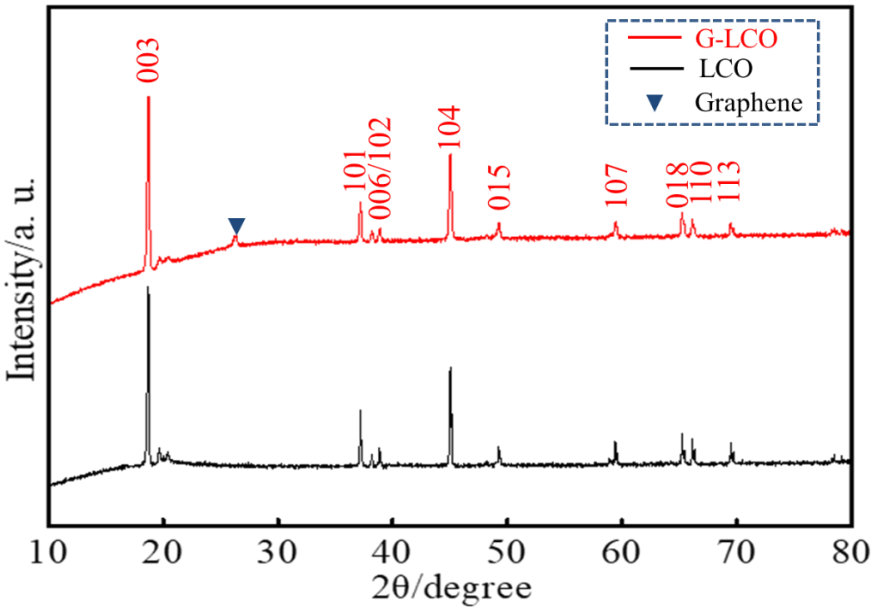

Figure 1. XRD patterns of the $LiCoO_2$ and G-LCO materials.

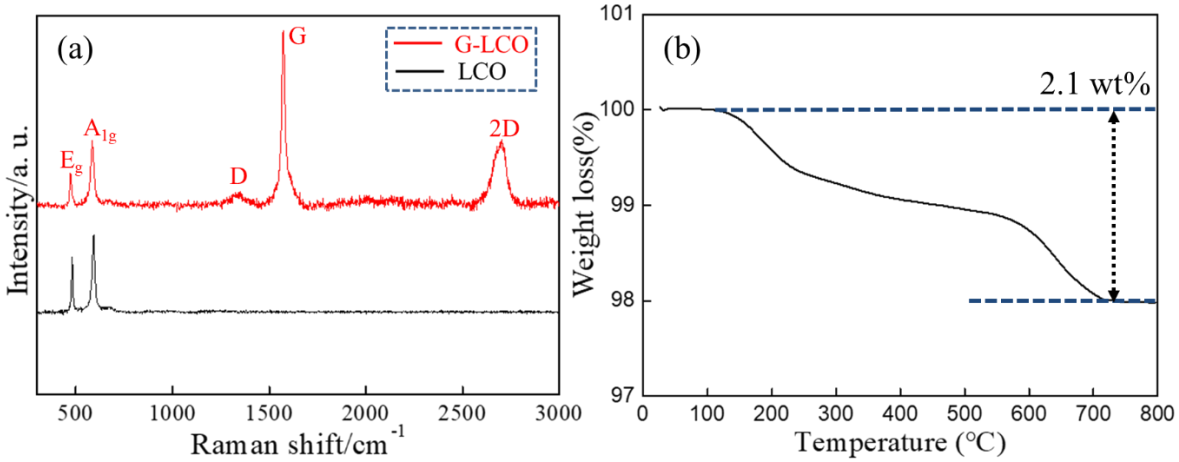

Figure 2. (a) Raman spectra of $LiCoO_2$ and G-LCO. (b) TGA curve of G-LCO.

The Raman spectra of both $LiCoO_2$ and G-LCO showed peaks at 482 and 598 cm^{-1} (Fig. 2a), attributed to the E_g and A_{1g} vibrations of layered oxide materials with an *R-3m* structure, respectively. For G-LCO, vibrations observed at 1350, 1572 and 2690 cm^{-1} are due to the D, G and 2D bands of

graphene, respectively. The results confirmed the existence of graphene nanosheets in G-LCO. To determine the amount of graphene in the G-LCO material, we used TGA to analyze the weight change in the temperature range from room temperature to 800°C (Fig. 2b). The mass loss that occurred between 140 and 240°C might be ascribed to the loss of oxygen-containing group in graphene nanosheets [51,52]. According to the TGA curve, the graphene content in G-LCO was approximately 2.1 wt%, which is very close to the design value.

Fig. 3(a) and (b) shows the typical morphologies of the as-prepared graphene nanosheets. FESEM and TEM images confirm that the graphene nanosheets are transparent in a typical size of 4–6 μm. The low-magnification image (Fig. 3c) of G-LCO reveals that the $LiCoO_2$ particles and graphene nanosheets are homogenously distributed in G-LCO composite without distinct aggregation, which can be attributed to the moderate and uniform coating process. Fig. 3d shows the typical FESEM image of G-LCO particles with high magnifications. The $LiCoO_2$ particles retained the shape of regular polyhedrons and graphene nanosheets are uniformly attached to the surface of $LiCoO_2$ particles. the boundary between $LiCoO_2$ particles and graphene nanosheets in the G-LCO composite is clear and distinguishable, showing a partial coating structure.

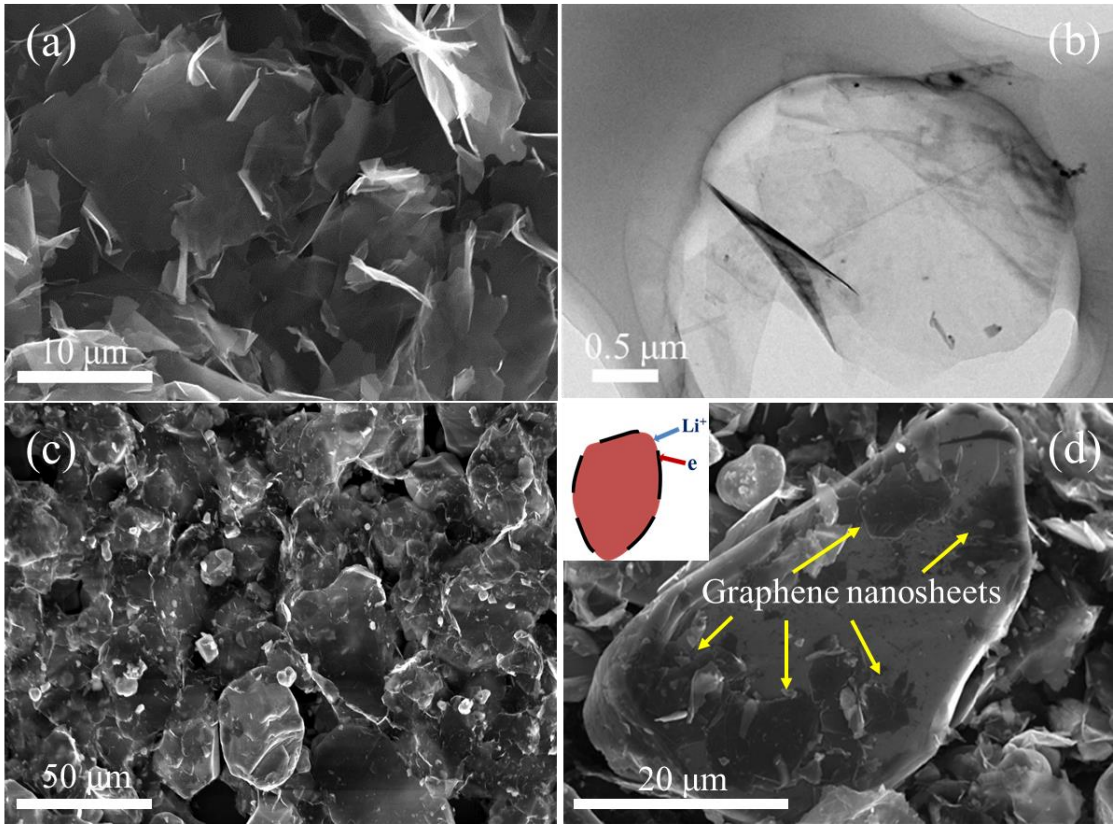

Figure 3. (a) FESEM and (b) TEM image of graphene nanosheets used in the experiments. FESEM images of G-LCO composite material under (c) 2000, (d)8000 times magnifications.

Accordingly, the ultrasonication and the slow evaporation process with continuous stirring can be helpful for the homogeneous distribution. The partial coating structure leaves a pathway for the Li^+

diffusion and provides an effective conducting network due to the excellent electronic conductivity of graphene, inducing promising electrochemical performance.

Fig. 4(a) and (b) show typical charge-discharge curves for different cycles of pristine $LiCoO_2$ and G-LCO electrodes in coin cells, respectively, at the 1st, 10th, 50th and 100th cycles at a current rate of 0.1 C (18 mA g^{-1}) between 2.5 and 4.5 V (vs. Li/Li^+). The initial charge and discharge capacity of $LiCoO_2$ electrode are 184.7 and 177.3 mAh g^{-1}, with a Columbic efficiency of approximately 95.9%. By contrast, the first charge and discharge capacities of the G-LCO electrode are 186.1 and 180.8 mAh g^{-1}, with a Coulombic efficiency of approximately 97.2%, which is higher than that of the pristine $LiCoO_2$ electrode. The larger reversible capacity of the G-LCO electrode can be attributed to the smaller polarization of the electrode, which increases the utilization of the active material. Besides, the initial irreversible capacity loss is partially contributed by the CEI formation due to the electrolyte decomposition at high voltage[28,29,53-55]. Fig. 8c presents the cycling performance of the pristine $LiCoO_2$ and G-LCO electrodes at 0.1C. The pristine $LiCoO_2$ electrode exhibited an initial discharge capacity of 177.3 mAh g^{-1}, and the discharge capacity was retained at 145.5 mAh g^{-1} after 100 cycles, with retention of 82.1%. In comparison, G-LCO electrode delivered an initial discharge capacity of 180.8 mAh g^{-1}, with a higher capacity retention of 88.5% in 100 cycles. At high operating voltage, coating with graphene could help to suppress the CEI layer formation at the electrode/electrolyte interface, thus improving the cycling stability of the electrode[56].

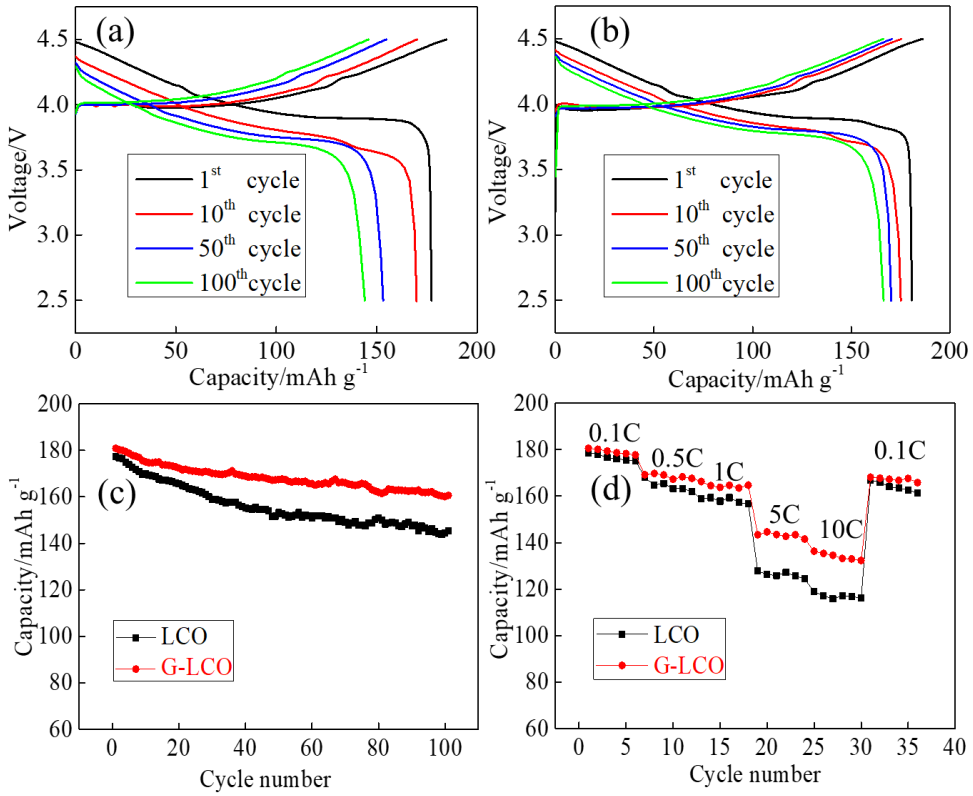

Figure 4. (a) Charge/discharge curves of the pristine $LiCoO_2$ at various cycle numbers at 0.1 C rate. (b) charge/discharge curves of the G-LCO electrode at various cycle numbers at 0.1 C rate. (c) cycling performance of pristine $LiCoO_2$ and G-LCO electrodes at 0.1C for 100 cycles. (b) rate performance of pristine $LiCoO_2$ and G-LCO electrodes charged at 0.1C and discharged at 0.1C-10C.

Moreover, as shown in Fig. 4a, at the 10th, 50th and 100th cycles, the voltage difference between charge and discharge increased with the cycling test, revealing a distinctive polarization growth of the pristine $LiCoO_2$ electrode. In contrast, the polarization growth for the G-LCO electrode in Fig. 4b was significantly mitigated, which indicates suppression of the side reactions by graphene nanosheets at the electrode surface. Fig. 4d compares the rate performance of the pristine $LiCoO_2$ and G-LCO electrodes by charging at 0.1C and discharging at different rates. The initial discharge capacity of the pristine $LiCoO_2$/G-LCO electrodes at 0.1, 0.5, 1, 5 and 10C was 178.6/180.6, 168.0/169.2, 158.8/166.3, 127.8/143.4, and 118.9/136.3 mAh g^{-1}, respectively. The better cycling stability and rate capability of the G-LCO electrode demonstrate that the designed partial coating structure with graphene nanosheets effectively improved the electrochemical properties of $LiCoO_2$ electrode. In addition, the performance comparison between some reported $LiCoO_2$ materials and the G-LCO material in this study is summarized in Table 1, which indicates that partial surface coating with graphene nanosheets showed significant improvement in comparison to most of the previous results listed.

Table 1. Performance comparison of G-LCO in this study with some reported $LiCoO_2$ materials.

Methods	Voltage (V)	Capacity at high rate (mAh g^{-1})	Capacity retention (%) (cycle number, rate)	Ref.
Al dopping	2.0-4.5	—	51 (9, 0.4 mA/cm^2)	57
Mn dopping	3.0-4.5	—	87.7 (50, 0.2 C)	58
Al_2O_3 coating	3.0-4.5	—	95(80,0.5C)	31
MgF_2 coating	3.0–4.5	105 (5 C)	80 (50, 0.2 C)	59
TiO_2 coating	2.75-4.4	—	81(100,0.2C)	33
Carbon coating	3.0-4.3	120(1C)	—	39
GQDs coating	3.0-4.5	105 (10 C)	83 (100, 0.5 C)	60
GN coating	2.5-4.5	136(10C)	88.5%(100, 0.1C)	Ours

GQDs: Graphene quantum dots, GN: graphene nanosheets.

To verify the effects of the partial coating structure by graphene nanosheets on the electrochemical properties of $LiCoO_2$, EIS measurements were performed for the pristine $LiCoO_2$ and G-LCO electrodes before cycling. As shown in Fig. 5a, both the $LiCoO_2$ and G-LCO electrodes have similar shapes of the Nyquist plots, including a high frequency semicircle (R_{sf}, attributed to the CEI film resistance of the $LiCoO_2$ electrode), a mediate frequency semicircle (R_{ct}, corresponding to the charge transfer resistance) and the inclined line associated with Li^+ diffusion through the cathode[61-63]. The kinetic differences between $LiCoO_2$ and G-LCO electrodes were investigated by modeling the electrochemical impedance spectra (EIS) based on the equivalent circuit (Fig. 5c). The fitted results of R_{sf} and R_{ct} are shown in Table 2.

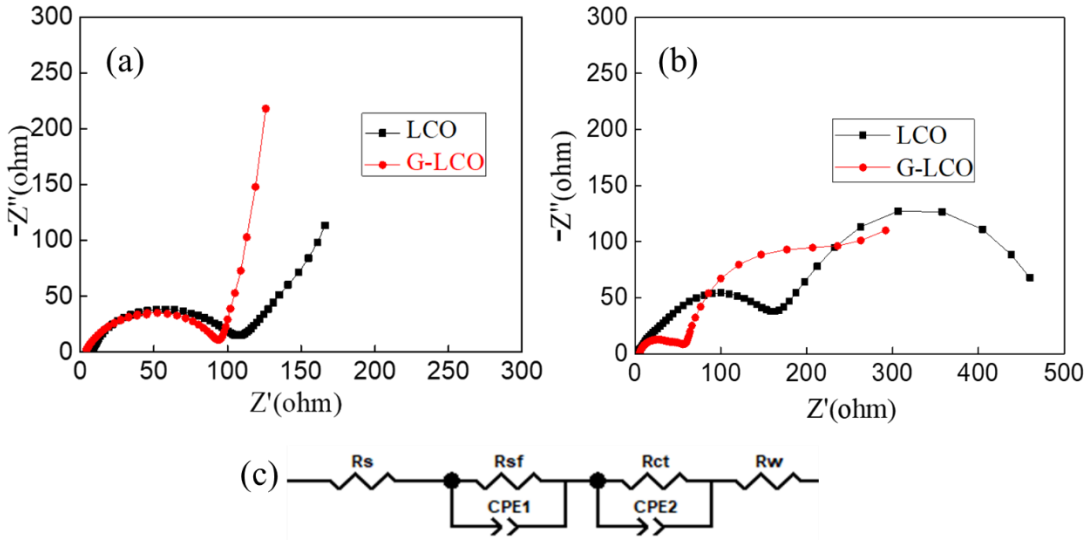

Figure 5. Nyquist plots of pristine $LiCoO_2$ and G-LCO electrodes: (a) before cycling, (b) after 100 cycles, and (c) the equivalent circuit diagram.

It can be seen that the charge transfer resistance of G-LCO electrode was 75.3 Ω, which was lower than $LiCoO_2$ electrode (91.5 Ω), indicating the partial coating structure can ensure the fast electron transport and Li^+ diffusion at the same time[45,64]. Therefore, an enhancement in the electrochemical kinetics induces the higher initial discharge capacity and better rate capability of G-LCO material[45,47,64]. After 100 cycles, the R_{sf} and R_{ct} values of $LiCoO_2$ electrode increase significantly, which could be ascribed to side reactions at cathode-electrolyte interface and gradual growth of CEI layer[29,54,60,65]. In contrast, the R_{sf} and R_{ct} values of G-LCO electrode both increase fairly slowly. It can be assumed that the increase of electrochemical impedance is greatly suppressed for G-LCO electrode. Thus, it can be deduced that the graphene nanosheets coated on the particle surface probably contributed to the suppression the interfacial side reactions and the reduction of the CEI growth under 4.5V cut-off voltage.

Table 2. Resistance values obtained from equivalent circuit fitting of EIS data of the $LiCoO_2$ and G-LCO electrodes

Samples	before cycling		100^{th} cycle	
	$R_{sf}(\Omega)$	$R_{ct}(\Omega)$	$R_{sf}(\Omega)$	$R_{ct}(\Omega)$
LCO	16.3	97.5	162.8	286.9
G-LCO	12.4	75.3	55.6	162.7

To further investigate the effect of graphene coating on CEI growth, XPS measurements were performed for the $LiCoO_2$ and G-LCO electrodes after 100 cycles. Fig. 6 shows the XPS spectra of Co 2p and O 1s at different etching depth of 0, 10nm, 20nm and 30nm for the $LiCoO_2$ and G-LCO electrodes after 100 cycles. Considering the limited probe depth of XPS, the relative intensity of the Co 2p and O

1s peak at different depths may indicate the CEI thickness[29]. As for Co 2p spectra of $LiCoO_2$ and G-LCO electrodes, the peak intensity was weak at the etching depth of 0 nm and 10 nm, which suggests the presence of the CEI layer on the surface of the electrodes.

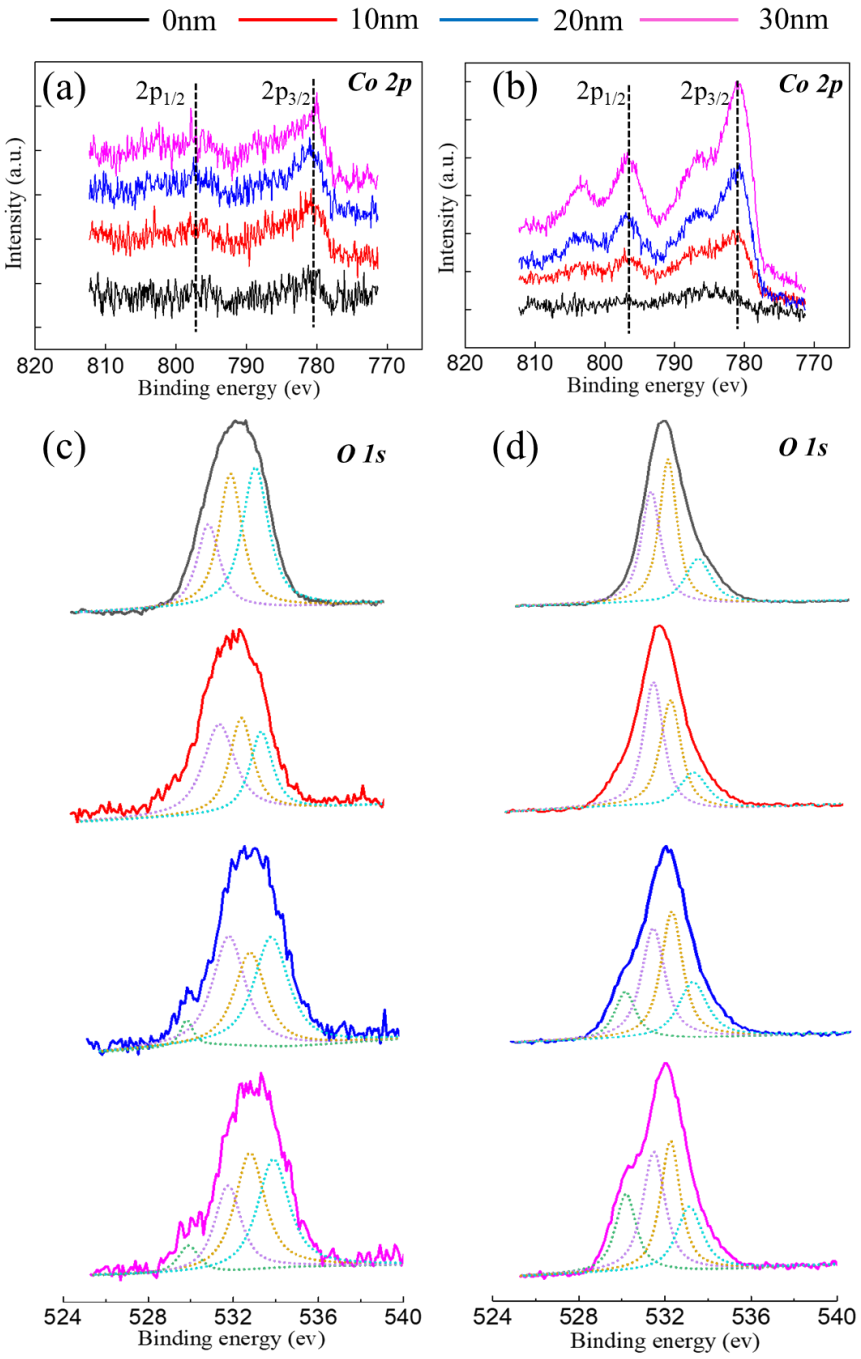

Figure 6. The Co 2p XPS spectra of (a) the pristine $LiCoO_2$ and (b) G-LCO electrodes after 100 cycles at different etching depths. The O 1s XPS spectra of (c) the pristine $LiCoO_2$ and (d) G-LCO electrodes after 100 cycles at different etching depths.

When the etching depth gradually increased to 20 and 30 nm respectively, the peaks representing $LiCoO_2$ material were identifiable for G-LCO, while these peaks were still very weak for the $LiCoO_2$

electrode. Therefore, the results indicate more severe CEI layer growth on the $LiCoO_2$ electrode than G-LCO electrode [66]. Regarding O 1s XPS spectra, the peak of lattice oxygen was reported to be located at 529.7 eV, while the peak around 531-535 eV was used to verify the existence of CEI layer [67]. At the etching depth of 0 nm and 10 nm, the peaks of lattice oxygen disappeared for the $LiCoO_2$ and G-LCO electrodes. When the etching depth gradually increased to 20 and 30 nm, peaks of lattice oxygen became identifiable, which also confirms the presence of the CEI layer. However, compared to $LiCoO_2$ electrode, peaks of lattice oxygen gained more weight than peaks of species with C–O (in carbonate or OP(OR)3) and O–H bonds for G-LCO electrode, which indicates suppressed CEI formation on the surface of G-LCO electrode[19,28,29,54]. The results indicated that the G-LCO electrode with graphene nanosheets showed fewer interphase reactions and CEI growth than the $LiCoO_2$ electrode after cycling for 100 cycles at 0.1C.

4. CONCLUSIONS

In this study, we used small size graphene nanosheets to partially coat $LiCoO_2$ by a facile solution method, and investigated how graphene coating works in the enhancement of the electrochemical performance under 4.5V cut-off voltage. The results demonstrated that the G-LCO material exhibited better rate capability and cycling stability. The results of CV, EIS and XPS measurements revealed that graphene modification contributed to the suppression of the CEI layer formation and enhanced the electrochemical reaction kinetics during the charge-discharge processes. This study demonstrated that partial coating with graphene nanosheets is an effective way to enhance the rate capability and cycling stability of the $LiCoO_2$ materials.

ACKNOWLEDGEMENT
This work was supported by grants from the Program of Graphene Special Innovative Fund of AECC Beijing Institute of Aeronautical Materials. We would like to thank Editage (www.editage.cn) for English language editing.

References

1. K. Sekai, H. Azuma, A. Omaru, S. Fujita, H. Imoto, T. Endo, K. Yamaura, Y. Nishi, S. Mashiko and M. Yokogawa, *Journal of Power Sources*, 43(1993) 241.
2. Z. S. Peng, C. R. Wan and C. Y. Jiang, *Journal of Power Sources*, 72(1998) 215.
3. Y. K. Sun, J. M. Han, S. T. Myung, S. W. Lee and K. Amine, *Electrochemistry Communications*, 8(2006) 821.
4. G. G. Amatucci, J. M. Tarascon and L. C. Klein, *Journal of The Electrochemical Society*,143(1996) 1114.
5. R. Yazami, Y. Ozawa, H. Gabrisch and B. Fultz, *Electrochimica Acta*, 50(2004) 385.
6. C. Delmas, M. Ménétrier, L. Croguennec, I. Saadoune, A. Rougier, C. Pouillerie, G. Prado, M. Grüne and L. Fournès, *Electrochimica Acta*, 45(1999) 243.
7. T. Ohzuku and A. Ueda, *Journal of The Electrochemical Society*, 141(1994) 2972.
8. J. M. Tarascon and M. Armand, *Nature*, 414(2001) 359.
9. M. Winter, J. O. Besenhard, M. E. Spahr and P. Novák, *Advanced Materials*,10(1998) 725.
10. S. Oh, J. K. Lee, D. Byun, W. I. Cho and B. Won Cho, *Journal of Power Sources*, 132(2004) 249.
11. D. D. MacNeil and J. R. Dahn, *Journal of The Electrochemical Society*, 149(2002), A912.

12. M. S. Whittingham, *ChemInform*, 35(2004) 4271.
13. H. Wang, E. Rus, T. Sakuraba, J. Kikuchi, Y. Kiya and H. D. Abruña, *Analytical Chemistry*, 86(2014) 6197.
14. J. B. Goodenough and K.-S. Park, *Journal of the American Chemical Society*, 135(2013) 1167.
15. J. Cho, Y. J. Kim and B. Park, *Journal of The Electrochemical Society*, 148(2001) A1110.
16. H. Wang, Y. I. Jang, B. Huang, D. R. Sadoway and Y. M. Chiang, *Journal of The Electrochemical Society*,146(1999) 473.
17. J. Xie, J. Zhao, Y. Liu, H. Wang, C. Liu, T. Wu, P.-C. Hsu, D. Lin, Y. Jin and Y. Cui, *Nano Research*, 10(2017) 3754.
18. L. Dahéron, R. Dedryvère, H. Martinez, M. Ménétrier, C. Denage, C. Delmas and D. Gonbeau, *Chemistry of Materials*, 20(2008) 583.
19. K. Xu, *Chemical Reviews*,114(2014) 11503.
20. N.-S. Choi, J.-G. Han, S.-Y. Ha, I. Park and C.-K. Back, *ChemInform*, 46(2015) 2372.
21. D. Aurbach, B. Markovsky, G. Salitra, E. Markevich, Y. Talyossef, M. Koltypin, L. Nazar, B. Ellis and D. Kovacheva, *Journal of Power Sources*, 165(2007) 491.
22. M. Gauthier, T. J. Carney, A. Grimaud, L. Giordano, N. Pour, H.-H. Chang, D. P. Fenning, S. F. Lux, O. Paschos, C. Bauer, F. Maglia, S. Lupart, P. Lamp and Y. Shao-Horn, *The Journal of Physical Chemistry Letters*, 6(2015) 4653.
23. Y. Qian, P. Niehoff, M. Börner, M. Grützke, X. Mönnighoff, P. Behrends, S. Nowak, M. Winter and F. M. Schappacher, *Journal of Power Sources*, 329(2016) 31.
24. M. G. S. R. Thomas, P. G. Bruce and J. B. Goodenough, *Solid State Ionics*, 17(1985) 13.
25. T. Tamura, M. Kohyama and S. Ogata, *Physical Review B*, 96(2017) 035107.
26. X. Zeng, G.-L. Xu, Y. Li, X. Luo, F. Maglia, C. Bauer, S. F. Lux, O. Paschos, S.-J. Kim, P. Lamp, J. Lu, K. Amine and Z. Chen, *ACS Applied Materials & Interfaces*, 8(2016) 3446.
27. W. Lu, J. Zhang, J. Xu, X. Wu and L. Chen, *ACS Applied Materials & Interfaces*, 9(2017) 19313.
28. G. Cherkashinin, K. Nikolowski, H. Ehrenberg, S. Jacke, L. Dimesso and W. Jaegermann, *Physical Chemistry Chemical Physics*, 14(2012) 12321.
29. J.-N. Zhang, Q. Li, Y. Wang, J. Zheng, X. Yu and H. Li, *Energy Storage Materials*,14(2018) 1.
30. L. Liu, L. Chen, X. Huang, X.-Q. Yang, W.-S. Yoon, H. S. Lee and J. McBreen, *Journal of The Electrochemical Society*, 151(2004) A1344.
31. D. Zuo, G. Tian, D. Chen, H. Shen, C. Lv, K. Shu and Y. Zhou, *Electrochimica Acta*, 178(2015) 447.
32. A. T. Appapillai, A. N. Mansour, J. Cho and Y. Shao-Horn, *Chemistry of Materials*, 19(2007) 5748.
33. G. Ting-Kuo Fey, C.-Z. Lu, T. Prem Kumar and Y.-C. Chang, *Surface and Coatings Technology*,199(2005) 22.
34. Z. Chen and J. R. Dahn, *Electrochimica Acta*, 49(2004) 1079.
35. H. C. Shin, W. I. Cho and H. Jang, *Journal of Power Sources*, 159(2006) 1383.
36. C. H. Mi, X. B. Zhao, G. S. Cao and J. P. Tu, *ChemInform*, 36(2005) A483.
37. H. Takahara, T. Takeuchi, M. Tabuchi, H. Kageyama, Y. Kobayashi, Y. Kurisu, S. Kondo and R. Kanno, *Journal of The Electrochemical Society*,151(2004) A1539.
38. J. Kim, B. Kim, J.-G. Lee, J. Cho and B. Park, *Journal of Power Sources*, 139(2005) 289.
39. Q. Cao, H. P. Zhang, G. J. Wang, Q. Xia, Y. P. Wu and H. Q. Wu, *Electrochemistry Communications*, 9(2007) 1228.
40. S. Sharifi-Asl, F. A. Soto, T. Foroozan, M. Asadi, Y. Yuan, R. Deivanayagam, R. Rojaee, B. Song, X. Bi, K. Amine, J. Lu, A. Salehi-khojin, P. B. Balbuena and R. Shahbazian-Yassar, *Advanced Functional Materials*, 29(2019) 1901110.
41. A. K. Geim and K. S. Novoselov, *Nature Materials*, 6(2007) 183.
42. W. Lv, D.-M. Tang, Y.-B. He, C.-H. You, Z.-Q. Shi, X.-C. Chen, C.-M. Chen, P.-X. Hou, C. Liu

and Q.-H. Yang, *ACS Nano*,3(2009) 3730.
43. F.-Y. Su, Y.-B. He, B. Li, X.-C. Chen, C.-H. You, W. Wei, W. Lv, Q.-H. Yang and F. Kang, *Nano Energy*, 1(2012) 429.
44. W. Lv, Z. Li, Y. Deng, Q.-H. Yang and F. Kang, *Energy Storage Materials*, 2(2016) 107.
45. W. Wei, W. Lv, M.-B. Wu, F.-Y. Su, Y.-B. He, B. Li, F. Kang and Q.-H. Yang, *Carbon*, 57(2013) 530.
46. T. Liu, S. Sun, Z. Zang, X. Li, X. Sun, F. Cao and J. Wu, *RSC Advances*, 7(2017) 20882.
47. R. Tang, Q. Yun, W. Lv, Y.-B. He, C. You, F. Su, L. Ke, B. Li, F. Kang and Q.-H. Yang, *Carbon*, 103(2016) 356.
48. J. Ha, S.-K. Park, S.-H. Yu, A. Jin, B. Jang, S. Bong, I. Kim, Y.-E. Sung and Y. Piao, *Nanoscale*, 5(2013) 8647.
49. Y. Shi, L. Wen, S. Pei, M. Wu and F. Li, *Journal of Energy Chemistry*, 30(2019) 19.
50. Y. Hernandez, V. Nicolosi, M. Lotya, F. M. Blighe, Z. Sun, S. De, I. T. McGovern, B. Holland, M. Byrne, Y. K. Gun'Ko, J. J. Boland, P. Niraj, G. Duesberg, S. Krishnamurthy, R. Goodhue, J. Hutchison, V. Scardaci, A. C. Ferrari and J. N. Coleman, *Nature Nanotechnology*, 3(2008) 563.
51. K. Zhang, L. L. Zhang, X. S. Zhao and J. Wu, *Chemistry of Materials*, 22(2010) 1392.
52. B. Song, M. O. Lai, Z. Liu, H. Liu and L. Lu, *Journal of Materials Chemistry A*, 1(2013) 9954.
53. D. Takamatsu, Y. Koyama, Y. Orikasa, S. Mori, T. Nakatsutsumi, T. Hirano, H. Tanida, H. Arai, Y. Uchimoto and Z. Ogumi, *Angewandte Chemie*, 124(2012) 11765.
54. T. Minato, H. Kawaura, M. Hirayama, S. Taminato, K. Suzuki, N. L. Yamada, H. Sugaya, K. Yamamoto, K. Nakanishi, Y. Orikasa, H. Tanida, R. Kanno, H. Arai, Y. Uchimoto and Z. Ogumi, *The Journal of Physical Chemistry C*, 120(2016) 20082.
55. N. Liu, H. Li, Z. Wang, X. Huang and L. Chen, *Electrochemical and Solid State Letters*, 9(2006) A328.
56. X. Tang, S. S. Jan, Y. Qian, H. Xia, J. Ni, S. V. Savilov and S. M. Aldoshin, *Scientific Reports*, 5(2015) 11958.
57. Y.-I. Jang, *Journal of The Electrochemical Society*, 146(1999) 862.
58. M. Zou, M. Yoshio, S. Gopukumar and J.-i. Yamaki, *ChemInform*, 35(2004).
59. Y. Bai, K. Jiang, S. Sun, Q. Wu, X. Lu and N. Wan, *Electrochimica Acta*, 134(2014) 347.
60. Y. Sun, H. Dong, K. Wu, X. Chen, S. Wang, W. Gu, Z. Hong, M. Liu, Y. Shen and W. Lu, *Journal of Electroanalytical Chemistry*, 866(2020) 114109.
61. A. Yano, M. Shikano, A. Ueda, H. Sakaebe and Z. Ogumi, *Journal of The Electrochemical Society*, 164(2017) A6116.
62. Z. Wang, Z. Wang, H. Guo, W. Peng, X. Li, G. Yan and J. Wang, *Journal of Alloys and Compounds*, 621(2015) 212.
63. S. Kim, S. Choi, K. Lee, G. J. Yang, S. S. Lee and Y. Kim, *Physical Chemistry Chemical Physics*, 19(2017) 4104.
64. J.-r. He, Y.-f. Chen, P.-j. Li, Z.-g. Wang, F. Qi and J.-b. Liu, *RSC Advances*, 4(2014) 2568.
65. Y. Xie, H. Gao, J. Gim, A. T. Ngo, Z.-F. Ma and Z. Chen, *The Journal of Physical Chemistry Letters*, 10(2019) 589.
66. Y.-C. Lu, A. N. Mansour, N. Yabuuchi and Y. Shao-Horn, *Chemistry of Materials*, 21(2009) 4408.
67. S. Verdier, L. El Ouatani, R. Dedryvère, F. Bonhomme, P. Biensan and D. Gonbeau, *Journal of The Electrochemical Society*, 154(2007) A1088.